SUPPLEMENTAL MATERIAL

Supplemental Methods

Histology

After ice cold PBS perfusion, atria of donor hearts were removed. Ventricles were placed in 4% PFA overnight at 4°C. Hearts were then rinsed with PBS x 3 and placed in PBS at 4°C overnight. Hearts were then placed in histology cassettes for paraffin embedding and dehydrated in 70% ethyl alcohol. Tissues were paraffin embedded and 4 µm sections were cut and stained with H&E. Images were obtained with EVOS imaging system model FLc or an AxioScan Z1 (Carl Zeiss, Jena, Germany). After imaging, slides were scored in a blinded fashion by a trained cardiac pathologist (CYL) based on the 1990 and 2004 ISHLT cellular rejection guidelines [37].

Immunofluorescence

After ice cold PBS perfusion, ventricles were placed in 4% PFA overnight at 4°C. Hearts were rinsed with PBS x 3 and infiltrated with 30% sucrose (in PBS) overnight at 4°C. Hearts were embedded in O.C.T. (Fisher HealthCare Tissue Plus O.C.T. Compound Cat 4585) and frozen at -80°C. 10 or 30 µm sections were obtained using a Leica Cryostat. Sections were then washed in TBS and stained in 10% FBS in TBS-T (0.05% Tween-20) blocking solution with primary antibodies: anti-GFP 1:2000 (Abcam Cat# ab13970), anti-RFP 1:1000 (Rockland p/n: 600-401-379), anti-mouse CD45 1:200 (BD Pharmingen Cat# 550539), anti-mouse CD68 1:200 clone FA-11 (Biolegend Cat# 137002), anti-Ki-67 1:200 (Invitrogen Cat# 14-5698-82), CD8a (Cell Signaling Technology Cat# D4W2Z 1:200) overnight at 4°C in a humidified environment. For TUNEL staining, prior to primary antibody staining, Click-iT Plus TUNEL Assay with Alexa Fluor 647 dye Cat# C10619 was used followed by standard antibody staining as above. After washing, appropriate secondary antibodies were added to blocking buffer and sections were stained for 60 minutes at room temperature protected from light (Alexa Fluor 488 goat anti-chicken (Cat # A11039), Alexa Fluor 555 goat anti-rabbit (Cat # A21428), Alexa Fluor 647 goat anti-rat (Cat# A21247)). DAPI mounting, anti-fade solution (Vectashield Cat #H-1200) was added immediately prior to placement of no. 1.5 coverslips. Images were obtained with Zeiss LSM 700 confocal microscope installed on an AxioImager.M2 or an AxioScan Z1. Acquired images were processed using ZEN Blue and/or

Black or Imaris V9.5 (Oxford Instruments). When quantifying cells, 10 μm sections were used. Entire heart sections were imaged with a 20X objective lens using both tile and z-stack features. Z-stacks were collapsed, and tiles stitched in ZEN. Cells were counted when the antibody of interest co-localized with DAPI. When possible, entire heart sections were counted. For 3D reconstruction, 30 μm sections were imaged with a single 40X z-stack. For surface area, volume, and projection quantification, at least two 40X fields in at least two non-consecutive sections were used for each heart. When possible, between 10-20 donor $CCR2^-$ or $CCR2^+$ macrophages were averaged for each heart. To assess cellular projections, reconstructed images were rotated and only distinct projections that measured at least 10 μm were considered. In all cases, genotype identification was blinded to the observer.

Flow Cytometry

Single cell suspensions were generated from ice cold PBS perfused hearts by finely mincing and digesting ventricles in DMEM with Collagenase IV (Sigma C5138) 4500 U/mL in DMEM, Hyaluronidase 1 (Sigma H3506) 2400 U/mL in DMEM, and DNAse I (Sigma D4527-40KU) 6000 U/mL in DMEM for 45 minutes at 37°C. To deactivate the enzymes, samples were washed with HBSS that was supplemented with 2% FBS and 0.2% BSA and filtered through 40 μm cell strainers. Red blood cell lysis was performed with ACK lysis buffer (Thermo Fisher Scientific) for five minutes at room temperature. Samples were washed with DMEM and resuspended in 100 μL of FACS buffer (DPBS with 2% FBS and 2 mM EDTA). Cells were stained with monoclonal antibodies at 4°C for 30 minutes in the dark. A complete list of antibodies is provided below. Samples were washed in FACS buffer and final resuspension was made in 300 μL FACS buffer. DAPI was used for identification of dead cells. Immune cells were first gated as $CD45^+$ followed by standard doublet exclusion. For single cell RNA sequencing sorting, flow cytometric analysis and sorting were performed on a BD FACS ARIAIII platform. Cells were first gated as $CD11b^+$ and then all $Ly6C^+$ and $CD64^+$ cells were further assessed. Donor (GFP^+) and recipient (GFP^-) cells were sorted separately. Donor macrophages were identified as $CD45^+$ $CD11b^+$ $Ly6c^-$ $CD64^+$ GFP^+ and then classified as alive ($DAPI^-$) or dead ($DAPI^+$). Spleens were pressed through 40 μM cell strainers and rinsed with DMEM. They were not further digested. Preparation was otherwise

identical to heart single cell suspension/staining. Cell death flow cytometric analyses were performed on BD FACS Melody.

Antibody	Source	Identifier
CD45-PerCP/Cyanine 5.5, clone 30-F11	Biolegend	Cat 103132
CD11b-PE/Cy7, clone M1/70	Biolegend	Cat 101215
Ly6c-BV510, clone HK1.4	Biolegend	Cat 128033
CD64-APC, clone X54-5/7.1	Biolegend	Cat 139305
CD192 (CCR2)-PE, clone SA203G11	Biolegend	Cat 150609
I-A/I-E- APC/Cy7, clone M5/114.15.2	Biolegend	Cat 107627
Ly6g- PE/Cy7, clone 1A8	Biolegend	Cat 127617
CD11b- BV785, clone M1/70	Biolegend	Cat 101243
DAPI	BD Biosciences	Cat 564907

Single Cell Analysis

Pre-processing: Sequencing alignment and de-multiplexing was performed using Cell Ranger from 10X Genomics to generate feature barcoded count matrices. All subsequent analysis was performed using the Seurat v4.0.0 package. The following quality control steps were performed to filter the count matrices: 1) genes expressed in fewer than 3 cells and cells expressing fewer than 200 genes were removed; 2) cells expressing > 5,000 genes and > 50,000 counts were discarded as these could be potential multiplet events; 3) cells with > 10% mitochondrial content were filtered out as these were deemed to be of low-quality. Normalization and variance-stabilization of raw counts was performed using SCTransform to find 3,000 variably expressed genes and percentage mitochondrial reads were regressed out. Principle component analysis was used to find nearest neighbors and a 2D UMAP embedding was used for visualization. Harmony was used to integrate data across different libraries. Differential gene expression testing was performed using the FindAllMarkers function between conditions and across clusters. Statistically significant genes (adjusted p-value < 0.05, Bonferroni correction) were used for over-representation pathway analysis using the clusterProfiler R package and WikiPathways database.

Trajectory analysis: Palantir in Python v3 was used to perform trajectory analysis in the recipient population. SCTransformed counts with mitochondrial counts and cell cycle state regressed out were used as the input. Monocytes were specified as the starting population and default parameters were used to infer pseudotime and entropy values.

MyD88 post-transplant day 3 reference mapping: The MyD88 post-transplant day 3 WT and KO datasets were processed using the same framework outlined in “pre-processing”. Differential Gene expression was used to annotate cell types a priori without reference mapping. SCTransform normalized data was also mapped onto the integrated recipient object using FindTransferAnchors() by projecting the PCA structure of the recipient onto the query dataset. Finally, MapQuery() was used to project the query dataset onto the recipient UMAP embedding to annotate query cell types from the recipient annotations. Reference mapped cell-type prediction scores were used to assess the robustness of label transfer.

Supplemental Figures

Figure S1:

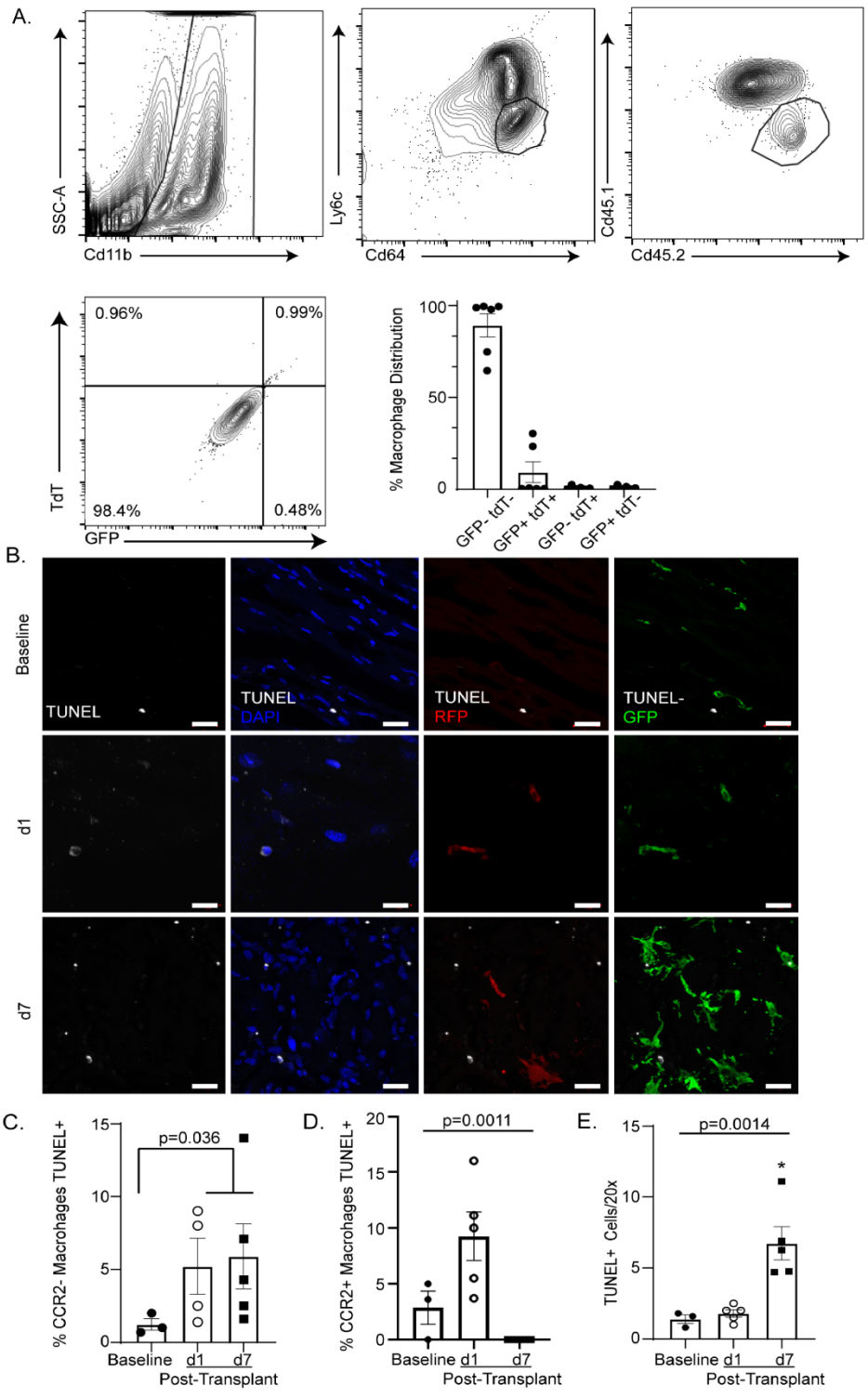
A.
SSC-A
Cd11b
Ly6c
Cd64
Cd45.1
Cd45.2
0.96%
0.99%
98.4%
0.48%
TdT
GFP
% Macrophage Distribution
100
50
0
GFP- tdT-
GFP+ tdT+
GFP- tdT+
GFP+ tdT-
B.
Baseline
d1
d7
TUNEL
TUNEL
DAPI
TUNEL
RFP
TUNEL-
GFP
C.
% CCR2- Macrohages TUNEL+
p=0.036
15
10
5
0
Baseline
d1
d7
Post-Transplant
D.
% CCR2+ Macrohages TUNEL+
p=0.0011
20
15
10
5
0
Baseline
d1
d7
Post-Transplant
E.
TUNEL+ Cells/20x
p=0.0014
*
15
10
5
0
Baseline
d1
d7
Post-Transplant

Figure S1: Donor Macrophages Undergo Cell Death after Heart Transplantation. A) B6 $CCR2^{ertCre/+}$ $Rosa26^{tdTomato}$ $CCR2^{GFP/+}$ CD45.2 mice were transplanted into CD45.1 BALB/c recipients and post-transplant day 7 hearts were gated on $CD45.2^{+}$ $CD11b^{+}$ $Ly6c^{-}$ $CD64^{+}$ with doublet exclusion (not shown) and assayed for double positive (GFP^{+} tdT^{+}), double negative (GFP^{-} tdT^{-}), or single positive (GFP^{+} or tdT^{+}) donor macrophages. Quantification showed the majority of donor macrophages were $CCR2^{-}$ (GFP^{-} TdT^{-}; 89.17%, n=6 hearts) or $CCR2^{+}$ (9.19%), with a minority expressing tdT^{+} but not GFP (0.75%) or expressing GFP only (0.87%) (Kruskal-Wallis; $p = 0.0031$). B) TUNEL immunofluorescence of donor $CCR2^{+}$ and $CCR2^{-}$ macrophages at baseline, post-transplant day 1 (d1), and post-transplant day 7 (d7) showing TUNEL (column 1), TUNEL and DAPI (column 2), TUNEL and RFP (column 3), and TUNEL and GFP (column 4). C) The percentage of donor $CCR2^{-}$ macrophages that are $TUNEL^{+}$ increase after transplant (baseline versus combined d1 and d7; Mann Whitney U Test; $p = 0.0364$, baseline n = 3, d1 = 4, d7 = 5). D) The percentage of donor $CCR2^{+}$ macrophages that are $TUNEL^{+}$ increase after transplant (Kruskal-Wallis; $p = 0.0011$). There were few donor $CCR2^{+}$ macrophages remaining at d7 (baseline n = 3, d1 = 5, d7 = 5). E) Quantification of total $TUNEL^{+}$ cells (DAPI and $TUNEL^{+}$) per 20X field at baseline, d1, and d7 show increased cell death (Kruskal-Wallis; $p = 0.0014$) and baseline versus d7 (Dunn's test for multiple comparisons; $p = 0.0139$) (baseline n = 3, d1 = 5, d7 = 5). Scale bar = 20 μm.

Figure S2:

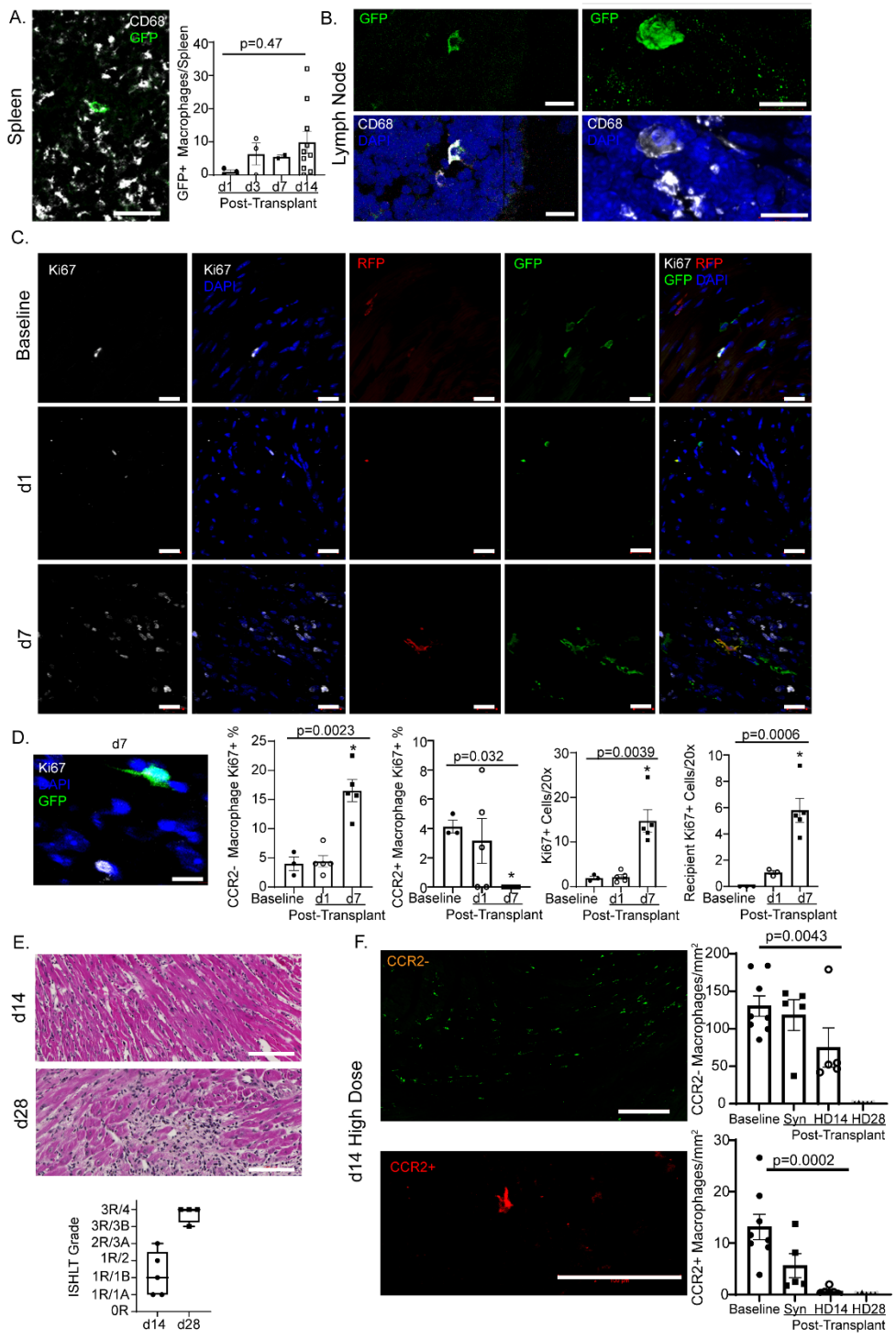
A.
Spleen
CD68
GFP
GFP+ Macrophages/Spleen
p=0.47
d1 d3 d7 d14
Post-Transplant
B.
Lymph Node
GFP
CD68
DAPI
C.
Baseline
d1
d7
Ki67
DAPI
RFP
GFP
Ki67 RFP
GFP DAPI
D.
d7
Ki67
DAPI
GFP
CCR2- Macrophage Ki67+ %
p=0.0023
CCR2+ Macrophage Ki67+ %
p=0.032
Ki67+ Cells/20x
p=0.0039
Recipient Ki67+ Cells/20x
p=0.0006
Baseline d1 d7
Post-Transplant
E.
d14
d28
ISHLT Grade
3R/4
3R/3B
2R/3A
1R/2
1R/1B
1R/1A
0R
d14 d28
F.
d14 High Dose
CCR2-
CCR2+
CCR2- Macrophages/mm²
p=0.0043
CCR2+ Macrophages/mm²
p=0.0002
Baseline Syn HD14 HD28
Post-Transplant

Figure S2: Donor Macrophages are Lost in the Setting of Ongoing Rejection. A) Immunofluorescent staining of donor CCR2$^-$ (CD68$^+$ GFP$^+$) macrophage in the recipient spleen. Quantification of donor macrophages by flow cytometry which showed no significant increase in donor macrophage (GFP$^+$) accumulation in the spleen after between post-transplant day 1 (d1) and post-transplant day 14 (d14) (Kruskal-Wallis; p = 0.47) (d1 n = 4, d3 = 3, d7 = 2, d14 = 10). B) Identification of rare donor CCR2$^-$ (CD68$^+$ GFP$^+$) macrophage in recipient lymph node. C-D) Donor CCR2$^-$ and CCR2$^+$ macrophages that co-labelled with Ki67$^+$ were considered proliferating (baseline n = 3, d1 = 5, d7 = 5). A greater percentage of CCR2$^-$ macrophages were proliferating after transplant (Kruskal-Wallis; p = 0.0023) and specifically at post-transplant day 7 (d7) compared to baseline (Dunn's test for multiple comparison; p = 0.034). The percentage of proliferating donor CCR2$^+$ macrophages decreased after transplant (Kruskal-Wallis; p = 0.032) and was significantly decreased at d7 (Dunn's test for multiple comparison; p = 0.042) compared to baseline. After transplant, there was an overall increase in proliferation of all cells (DAPI + Ki67) (Kruskal-Wallis; p = 0.0039) and significantly at d7 (Dunn's test for multiple comparison; p = 0.0382) compared to baseline. Recipient CD68$^+$ cells showed increased proliferation after transplant (Kruskal-Wallis; p = 0.0006) and specifically at d7 (Dunn's test for multiple comparison; p = 0.0071) compared to baseline (baseline n = 3, d1 = 3, d7 = 5). E) High-dose CTLA4-Ig was administered until d14. At d14 (n = 5), heart grafts were generally scored as mild cellular rejection (1R); however, grafts collected at post-transplant day 28 (d28, n = 4) were scored as severe cellular rejection (3R). F) High-dose CTLA4-Ig in an allogenic model or no immunosuppression in a syngeneic model were utilized to assess the effect of ischemic injury on donor macrophage dynamics. In the high-dose CTLA4-Ig cohort, at d14, similar numbers of donor CCR2$^-$ macrophages were identified compared to baseline (Dunn's test for multiple comparison; p = 0.52); however, a significant reduction of donor CCR2$^-$ macrophages were observed after cessation of CTLA4-Ig (baseline versus d28; Dunn's test for multiple comparison; p = 0.0018). In the syngeneic cohort, no difference was observed in the between post-transplant day 14 and baseline (Dunn's test for multiple comparison; p = 0.99). When comparing all groups, including post-transplant day 28 after cessation of CTLA4-Ig, there was a significant loss over time (Kruskal-Wallis; p =

0.0043). Compared to baseline, there was a significant loss of donor $CCR2^{+}$ macrophages at both d14 (Dunn's test for multiple comparison; p = 0.0082) and at d28 (Dunn's test for multiple comparison; p = 0.0001) in the high-dose CTLA4-Ig groups (baseline n = 8, d14 = 5, d28 = 4) but not the syngeneic group at post-transplant day 14 (n = 5; Dunn's test for multiple comparison; p = 0.71). When comparing all groups, including post-transplant day 28 after cessation of CTLA4-Ig, there was a significant loss over time (Kruskal-Wallis; p = 0.0002). Scale bar: A =40 μm, B-C = 10 μm, D = 20 μm, E = 100 μm, F (top) = 200 μm, F (bottom) = 100 μm.

Figure S3:

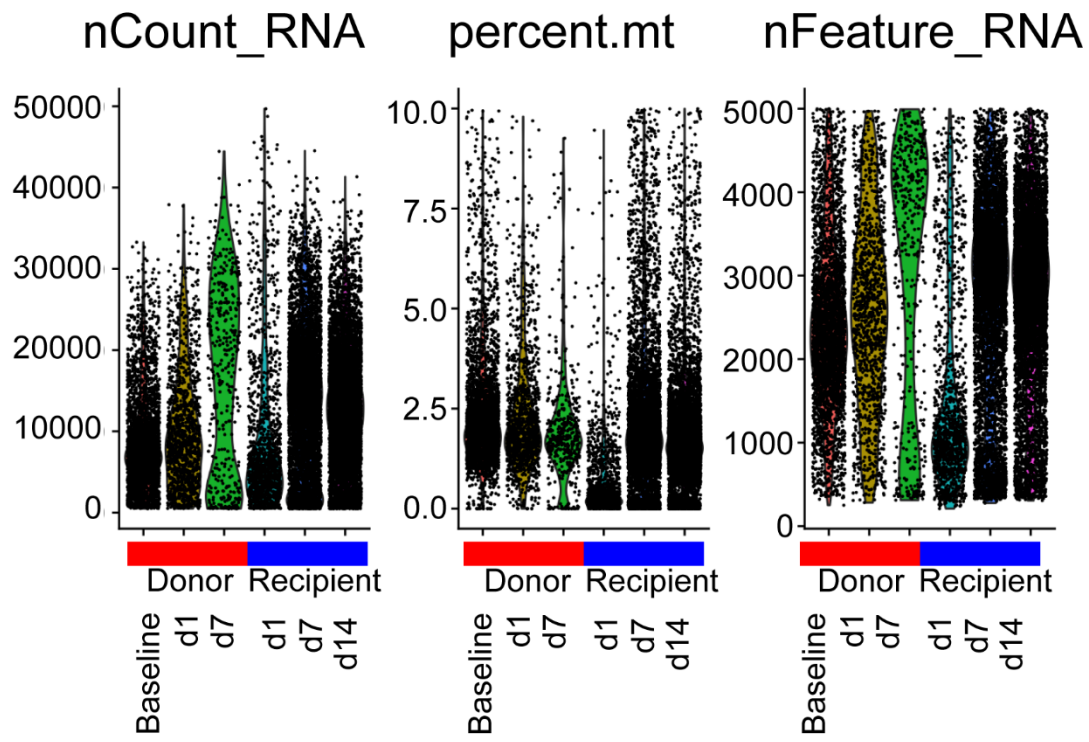

Quality control data plots showing RNA count, percent mitochondria, and feature counts of each population at baseline, post-transplant day 1 (d1), post-transplant day 7 (d7), and post-transplant day 14 (d14).

Figure S4:

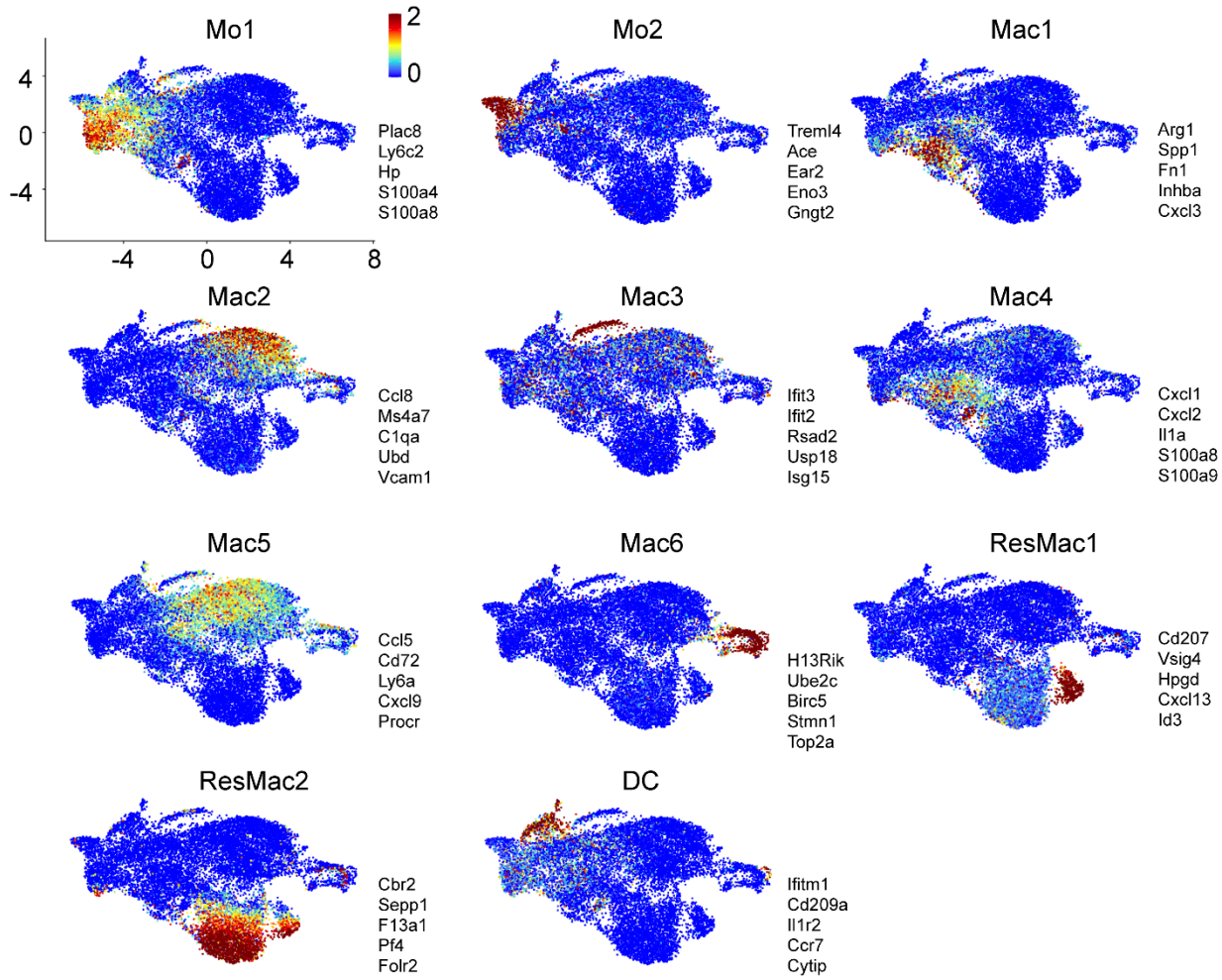
Mo1
2
0
4
0
-4
-4
0
4
8
Plac8
Ly6c2
Hp
S100a4
S100a8
Mo2
Treml4
Ace
Ear2
Eno3
Gngt2
Mac1
Arg1
Spp1
Fn1
Inhba
Cxcl3
Mac2
Ccl8
Ms4a7
C1qa
Ubd
Vcam1
Mac3
Ifit3
Ifit2
Rsad2
Usp18
Isg15
Mac4
Cxcl1
Cxcl2
Il1a
S100a8
S100a9
Mac5
Ccl5
Cd72
Ly6a
Cxcl9
Procr
Mac6
H13Rik
Ube2c
Birc5
Stmn1
Top2a
ResMac1
Cd207
Vsig4
Hpgd
Cxcl13
Id3
ResMac2
Cbr2
Sepp1
F13a1
Pf4
Folr2
DC
Ifitm1
Cd209a
Il1r2
Ccr7
Cytip

Figure S4: Diverse Gene Expression in Myeloid Populations. Combined z-score for top 5 statistically significant differentially expressed genes overlaid on UMAP embedding plot for Mo1 (Plac8, Ly6c2, Hp, S100a4, S100a8), Mo2 (Treml4, Ace, Ear2, Eno3, Gngt2), Mac1 (Arg1, Spp1, Fn1, Inhba, Cxcl3), Mac2 (Ccl8, Ms4a7, C1qa, Ubd, Vcam1), Mac3 (Ifit3, Ifit2, Rsad2, Usp18, Isg15), Mac4 (Cxcl1, Cxcl2, Il1a, S100a8, S100a9), Mac5 (Ccl5, Cd72, Ly6a, Cxcl9, Procr), Mac6 (2810417H13Rik, Ube2c, Birc5, Stmn1, Top2a), ResMac1 (Cd207, Vsig4, Hpgd, Cxcl13, Id3), ResMac2 (Cbr2, Sepp1, F13a1, Pf4, Folr2), DC (Ifitm1, Cd209a, Il1r2, Ccr7, Cytip).

Figure S5:

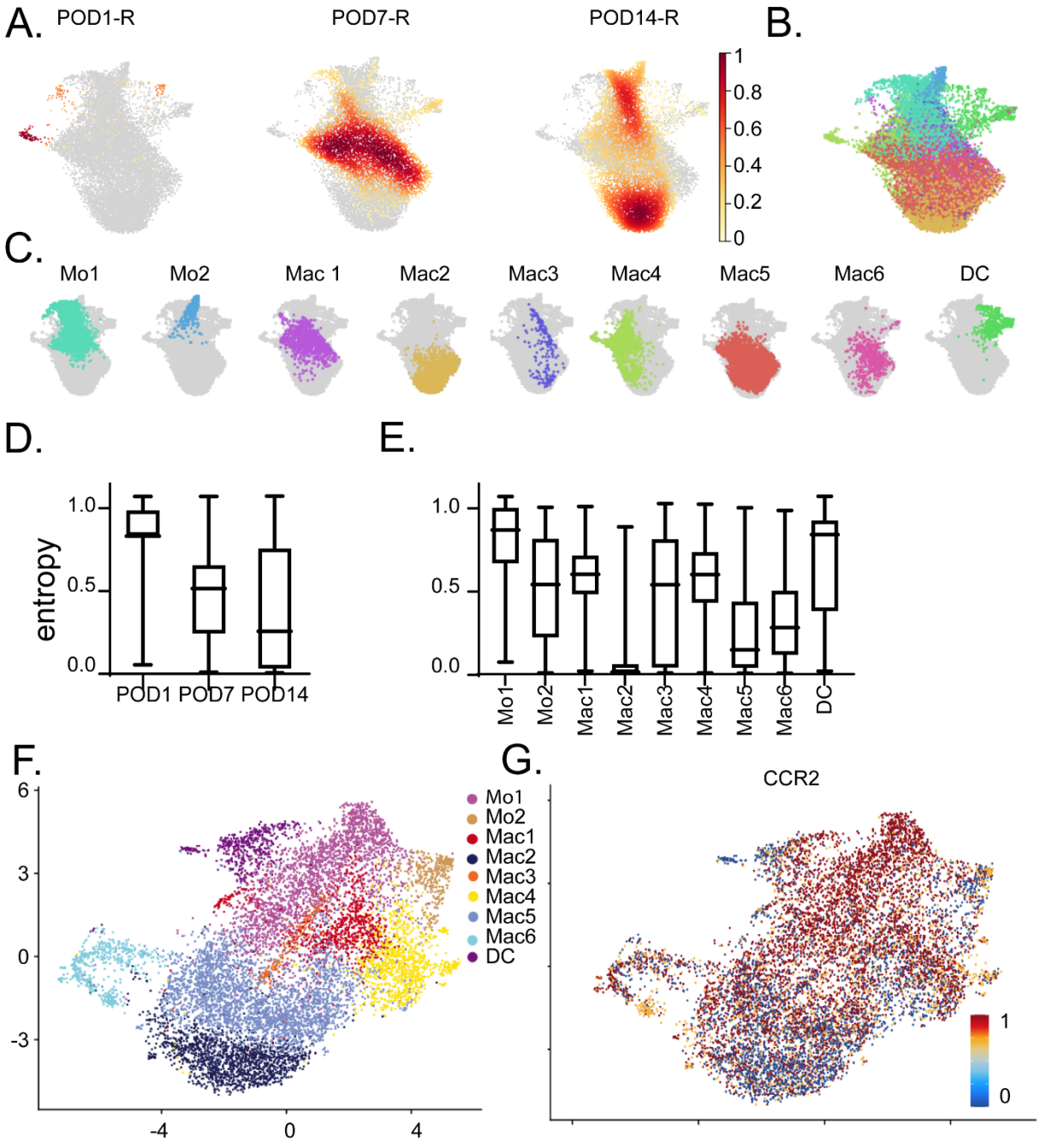
A.
POD1-R
POD7-R
POD14-R
1
0.8
0.6
0.4
0.2
0
B.
C.
Mo1
Mo2
Mac 1
Mac2
Mac3
Mac4
Mac5
Mac6
DC
D.
entropy
1.0
0.5
0.0
POD1 POD7 POD14
E.
1.0
0.5
0.0
Mo1
Mo2
Mac1
Mac2
Mac3
Mac4
Mac5
Mac6
DC
F.
6
3
0
-3
-4
0
4
Mo1
Mo2
Mac1
Mac2
Mac3
Mac4
Mac5
Mac6
DC
G.
CCR2
1
0

Figure S5: Recipient monocyte fate specification and diversity after heart transplantation.

A) Gaussian kernel density plots of post-transplant days 1, 7, and 14 cells in a force directed layout (FDL). B) FDL embedding colored by myeloid cell states. C) FDL embedding with each myeloid cell state highlighted. Palantir computed entropy split by (D) time point post-transplant and (E) myeloid cell states. (F) UMAP embedding plot colored my myeloid cell states. (G) Ccr2 RNA expression in UMAP space.

Figure S6:

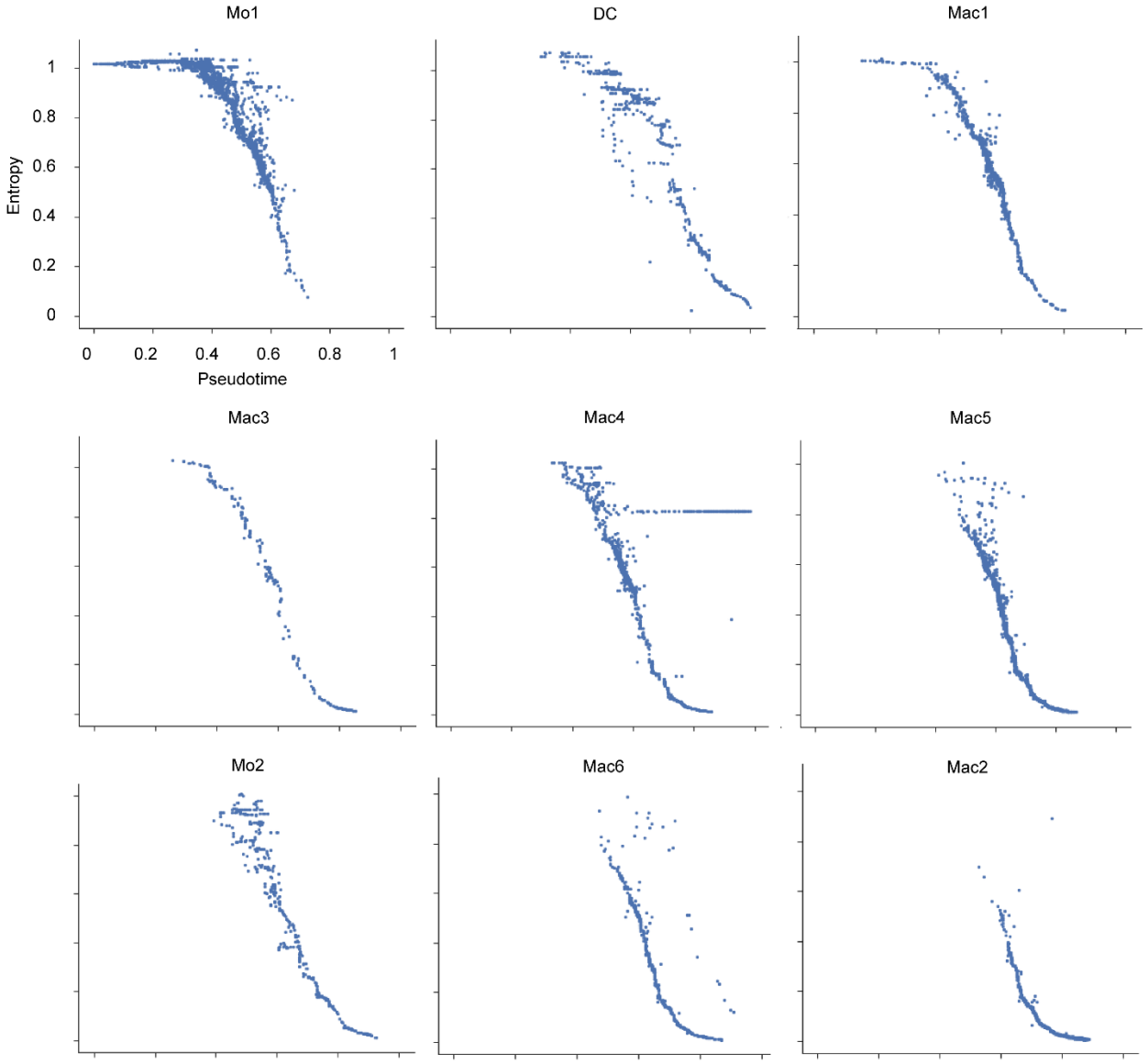
Mo1
DC
Mac1
Mac3
Mac4
Mac5
Mo2
Mac6
Mac2
Entropy
Pseudotime
0
0.2
0.4
0.6
0.8
1

Figure S6: Recipient Immune Cells Lose Entropy after Infiltrating Donor Heart. Recipient Palantir derived entropy versus pseudotime trajectories split by Mo1, DC, Mac1, Mac3, Mac4, Mac5, Mo2, Mac6, Mac2.

Figure S7:

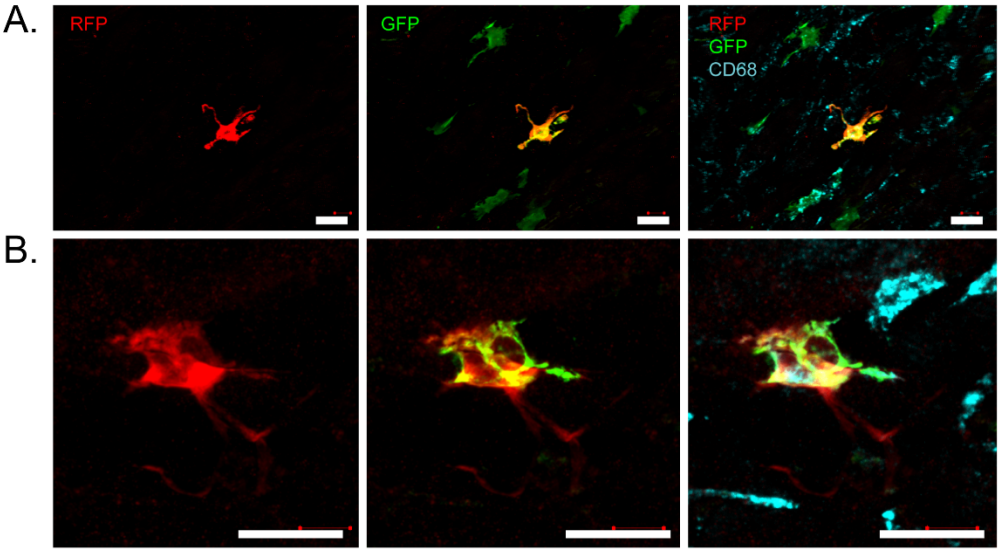
A.
RFP
GFP
RFP
GFP
CD68
B.

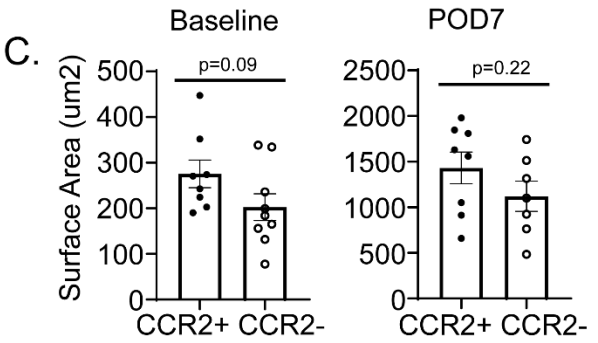
C.
Baseline
POD7
Surface Area (um2)
p=0.09
p=0.22
CCR2+ CCR2-
CCR2+ CCR2-

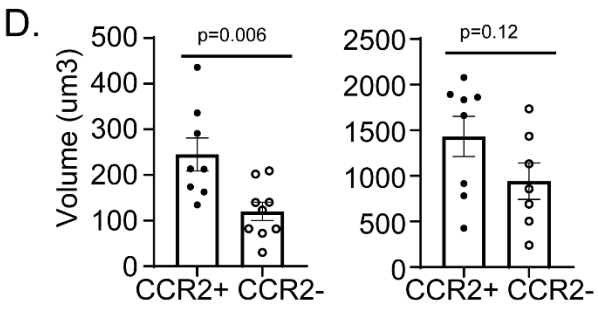
D.
Volume (um3)
p=0.006
p=0.12
CCR2+ CCR2-
CCR2+ CCR2-

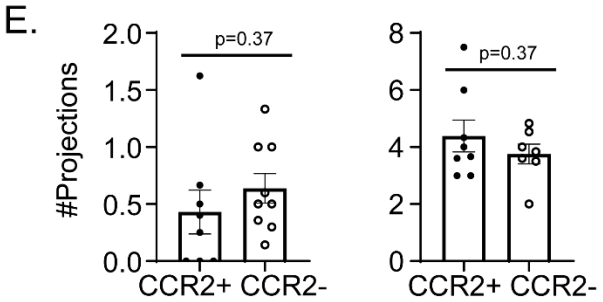
E.
#Projections
p=0.37
p=0.37
CCR2+ CCR2-
CCR2+ CCR2-

Figure S7: Donor Macrophages Dynamically Change after Transplant. A) At post-transplant day 7, donor $CCR2^-$ (GFP^+ RFP^-) macrophages surround a single donor $CCR2^+$ macrophage (GFP^+ RFP^+). B) At post-transplant day 7, a donor $CCR2^+$ macrophage is in proximity to recipient GFP^- RFP^- $CD68^+$ macrophages. C) There are no significant differences in surface area measurements between donor $CCR2^-$ macrophages and donor $CCR2^+$ macrophages at baseline (Mann-Whitney U Test; $p = 0.09$,) or at d7 (Mann-Whitney U Test; $p = 0.22$). D) Donor $CCR2^-$ macrophages have less volume than donor $CCR2^+$ macrophages at baseline (Mann-Whitney U Test; $p=0.006$) but there are no differences in volume noted at d7 (Mann-Whitney U Test; $p=0.12$). E) There are no between group differences between donor $CCR2^-$ and $CCR2^+$ macrophages in terms of number of projections at baseline (Mann-Whitney U Test; $p = 0.37$) or at d7 (Mann-Whitney U Test; $p = 0.37$) (baseline $CCR2^+$ $n = 8$, $CCR2^-$ $n = 9$; d7 $CCR2^+$ $n = 8$, $CCR2^-$ $n = 7$). Scale bar = 20 μm.

Figure S8:

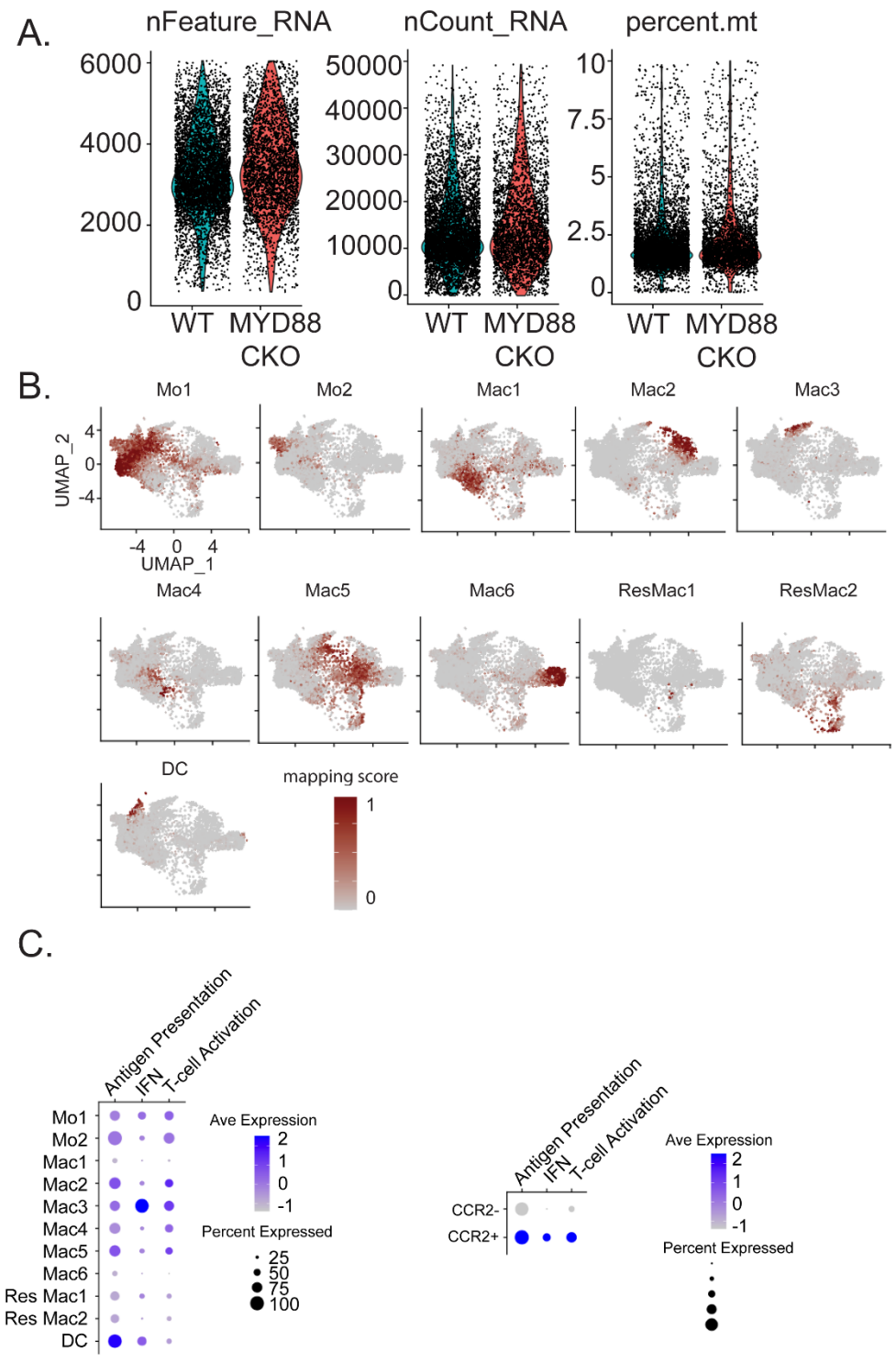
A.
nFeature_RNA
nCount_RNA
percent.mt
6000
4000
2000
0
50000
40000
30000
20000
10000
0
10
7.5
5
2.5
0
WT
MYD88 CKO
B.
Mo1
Mo2
Mac1
Mac2
Mac3
Mac4
Mac5
Mac6
ResMac1
ResMac2
DC
UMAP_2
UMAP_1
mapping score
1
0
C.
Antigen Presentation
IFN
T-cell Activation
Mo1
Mo2
Mac1
Mac2
Mac3
Mac4
Mac5
Mac6
Res Mac1
Res Mac2
DC
Ave Expression
2
1
0
-1
Percent Expressed
25
50
75
100
CCR2-
CCR2+

Figure S8: Single Cell RNA Sequencing of MyD88 CKO. A) Quality control data plots showing feature counts, RNA counts, and percent mitochondria for each population. B) Mapping scores of post-transplant day 3 composite mapped onto integrated UMAP for Mo1, Mo2, Mac1, Mac2, Mac3, Mac4, Mac5, Mac6, ResMac1, ResMac2, and DC. C. Dot plot split by cell state and CCR2 expression of antigen presentation, type II IFN, and T-cell activation signatures.